cea

# DAPNIA







DAPNIA-04-239 09/2004

## The Quasielastic $^3$He(e,e'p)d Reaction at $Q^2 = 1.5$ GeV$^2$ for Recoil Momenta up to 1 GeV/c

M.M. Rvachev et al (J.M. Laget)

*Submitted to Physical Review Letters*

**D**épartement d'**A**strophysique, de Physique des **P**articules, de Physique **N**ucléaire et de l'**I**nstrumentation **A**ssociée

DSM/DAPNIA, CEA/Saclay F - 91191 Gif-sur-Yvette Cédex
Tél : (1) 69 08 24 02 Fax : (1) 69 08 99 89
http : //www-dapnia.cea.fr

# The Quasielastic $^3$He$(e,e'p)d$ Reaction at $Q^2 = 1.5$ GeV$^2$ for Recoil Momenta up to 1 GeV/$c$

M. M. Rvachev,[1] F. Benmokhtar,[2,3] E. Penel-Nottaris,[4] K. A. Aniol,[5] W. Bertozzi,[1] W. U. Boeglin,[6] F. Butaru,[4] J. R. Calarco,[7] Z. Chai,[1] C. C. Chang,[8] J. -P. Chen,[9] E. Chudakov,[9] E. Cisbani,[10] A. Cochran,[11] J. Cornejo,[5] S. Dieterich,[2] P. Djawotho,[12] W. Duran,[5] M. B. Epstein,[5] J. M. Finn,[12] K. G. Fissum,[13] A. Frahi-Amroun,[3] S. Frullani,[10] C. Furget,[4] F. Garibaldi,[10] O. Gayou,[12] S. Gilad,[1] R. Gilman,[2,9] C. Glashausser,[2] J.-O. Hansen,[9] D. W. Higinbotham,[1,9] A. Hotta,[14] B. Hu,[11] M. Iodice,[10] R. Iomni,[10] C. W. de Jager,[9] X. Jiang,[2] M. K. Jones,[9,8] J. J. Kelly,[8] S. Kox,[4] M. Kuss,[9] J. M. Laget,[15] R. De Leo,[16] J. J. LeRose,[9] E. Liatard,[4] R. Lindgren,[17] N. Liyanage,[9] R. W. Lourie,[18] S. Malov,[2] D. J. Margaziotis,[5] P. Markowitz,[6] F. Merchez,[4] R. Michaels,[9] J. Mitchell,[9] J. Mougey,[4] C. F. Perdrisat,[12] V. A. Punjabi,[19] G. Quéméner,[4] R. D. Ransome,[2] J.-S. Réal,[4] R. Roché,[20] F. Sabatié,[21] A. Saha,[9] D. Simon,[21] S. Strauch,[2] R. Suleiman,[1] T. Tamae,[22] J. A. Templon,[23] R. Tieulent,[4] H. Ueno,[24] P. E. Ulmer,[21] G. M. Urciuoli,[10] E. Voutier,[4] K. Wijesooriya,[25] and B. Wojtsekhowski[9]

(The Jefferson Lab Hall A Collaboration)

[1] *Massachusetts Institute of Technology, Cambridge, Massachusetts 02139, USA*
[2] *Rutgers, The State University of New Jersey, Piscataway, New Jersey 08854, USA*
[3] *Université des Sciences et de la Technologie, BP 32, El Alia, Bab Ezzouar, 16111 Alger, Algérie*
[4] *Laboratoire de Physique Subatomique et de Cosmologie, F-38026 Grenoble, France*
[5] *California State University Los Angeles, Los Angeles, California 90032, USA*
[6] *Florida International University, Miami, Florida 33199, USA*
[7] *University of New Hampshire, Durham, New Hampshire 03824, USA*
[8] *University of Maryland, College Park, Maryland 20742, USA*
[9] *Thomas Jefferson National Accelerator Facility, Newport News, Virginia 23606, USA*
[10] *INFN, Sezione Sanitá and Istituto Superiore di Sanitá, Laboratorio di Fisica, I-00161 Rome, Italy*
[11] *Hampton University, Hampton, Virginia 23668, USA*
[12] *College of William and Mary, Williamsburg, Virginia 23187, USA*
[13] *University of Lund, Box 118, SE-221 00 Lund, Sweden*
[14] *University of Massachusetts, Amherst, Massachusetts 01003, USA*
[15] *CEA-Saclay, F-91191 Gif Sur-Yvette Cedex, France*
[16] *INFN, Sezione di Bari and University of Bari, I-70126 Bari, Italy*
[17] *University of Virginia, Charlottesville, Virginia 22901, USA*
[18] *State University of New York at Stony Brook, Stony Brook, New York 11794, USA*
[19] *Norfolk State University, Norfolk, Virginia 23504, USA*
[20] *Florida State University, Tallahassee, Florida 32306, USA*
[21] *Old Dominion University, Norfolk, Virginia 23529, USA*
[22] *Tohoku University, Sendai 980, Japan*
[23] *University of Georgia, Athens, Georgia 30602, USA*
[24] *Yamagata University, Kojirakawa-machi 1-4-12, Yamagata 990-8560, Japan*
[25] *University of Illinois at Urbana Champaign, Urbana, Illinois 61801, USA*

(Dated: September 7, 2004)

We have studied the quasielastic $^3$He$(e,e'p)d$ reaction in perpendicular coplanar kinematics, with the energy and momentum transferred by the electron fixed at 840 MeV and 1502 MeV/$c$, respectively. The $^3$He$(e,e'p)d$ cross section was measured for missing momenta up to 1000 MeV/$c$, while the $A_{TL}$ asymmetry was extracted for missing momenta up to 660 MeV/$c$. For missing momenta up to 150 MeV/$c$, the measured cross section is described well by calculations that use a variational ground-state wave function of the $^3$He nucleus derived from a potential that includes three-body forces. For missing momenta from 150 to 750 MeV/$c$, strong final-state interaction effects are observed. Near 1000 MeV/$c$, the experimental cross section is more than an order of magnitude larger than predicted by available theories. The $A_{TL}$ asymmetry displays characteristic features of broken factorization, and is described reasonably well by available models.

PACS numbers: 21.45.+v, 25.30.Dh, 27.10+h

The quasielastic $^3$He$(e,e'p)d$ reaction has been used to study the single-proton wave function in $^3$He. In the Plane-Wave Impulse Approximation (PWIA), this reaction samples the single-particle momentum distribution in the $^3$He nucleus. Thus, using modern Faddeev [1, 2] and variational [3] techniques to solve the non-relativistic three-body problem, one hopes to test the ability to predict the structure of three-body systems with state-of-the-art realistic NN potentials. However, final-state interactions (FSI), two-body currents (meson exchange and

isobar), as well as relativity have to be taken into account in the data interpretation, thus providing additional testing grounds for theoretical models. In extreme kinematics, the $^3$He$(e,e'p)d$ reaction can be used to probe the limits of single-particle models of the $^3$He structure [4].

High-energy electron beams with high currents and 100% duty factor at the Thomas Jefferson National Accelerator Facility (JLab) enable experiments to reach new kinematic domains and levels of precision in the study of $(e,e'p)$ reactions. In this Letter, we report on precision measurements [5] of the $^3$He$(e,e'p)d$ reaction in quasielastic kinematics that significantly extend the available data in both the transferred four-momentum, $Q^2$, and the recoil momentum of the undetected deuteron (missing momentum), $p_m$.

Measurements were performed using an incident beam of 4806 MeV and the two high-resolution spectrometer system (HRS) in Hall A of JLab. A detailed description of the Hall A instrumentation is available in [6]. Electrons (protons) where detected with the left (right) HRS respectively, HRS-L and HRS-R. Scattered electrons were detected at a central scattering angle of 16.4° and a central momentum of 3966 MeV/$c$, corresponding to the quasielastic knockout of protons from the $^3$He nucleus with transferred three-momentum $|\vec{q}| = 1502$ MeV/$c$, energy $\omega = 840$ MeV, four-momentum $Q^2 = 1.55$ GeV$^2$, and Bjorken scaling variable $x_B = Q^2/(2\omega M_p) = 0.98$. The ejected proton was detected in coincidence with the scattered electron in coplanar kinematics over a range of angles and momenta (see Table 1), to measure the $p_m$ dependence of the $^3$He$(e,e'p)d$ cross section on both sides of the momentum transfer, $\vec{q}$, direction.

TABLE I: Central kinematic values of the $^3$He$(e,e'p)d$ measurements. Listed are central settings of the hadron spectrometer (momentum $P_p$, angle $\theta_p$, and missing momentum $p_m$). Negative (positive) $p_m$ corresponds to the detected proton forward (backward) of $\vec{q}$. The electron kinematics were fixed, at incident and scattered electron energies of E=4806 MeV and E′=3966 MeV respectively, and scattering angle of $\theta_e$=16.4° ($Q^2$=1.55 GeV$^2$, $|\vec{q}|$=1502 MeV/$c$, $\omega$=840 MeV, $x_B$=0.98).

| $p_m$ MeV/$c$ | $P_p$ MeV/$c$ | $\theta_p$ deg |
|---|---|---|
| -550 | 1406 | 26.79 |
| -425 | 1444 | 31.84 |
| -300 | 1472 | 36.76 |
| -150 | 1493 | 42.56 |
| 0 | 1500 | 48.30 |
| 150 | 1493 | 54.04 |
| 300 | 1472 | 59.83 |
| 425 | 1444 | 64.76 |
| 550 | 1406 | 69.80 |
| 750 | 1327 | 78.28 |
| 1000 | 1171 | 89.95 |

A cooled, 10.3 cm diameter $^3$He gas target was used at temperature T = 6.3 K and pressures P = 8.30 - 10.9 atm, corresponding to densities $\rho$ = 0.0603 - 0.0724 g/cm$^3$. Relative changes in the target density were monitored by observing changes in the rate of singles events in the fixed HRS-L per unit beam charge passing through the target. The target density was determined by measuring the elastic $^3$He$(e,e)$ cross section at a beam energy of 644 MeV ($\theta_e = 30.7°$, $Q^2 = 2.91$ fm$^{-2}$), and normalizing it to the cross section derived from a fit to the world data of $^3$He elastic form factors [7]. The overall normalization uncertainty of the $^3$He density is estimated to be 2.9%, obtained as the quadratic sum of the systematic uncertainty of our $^3$He elastic cross section measurement (2.4%), the statistical uncertainty (0.5%), the uncertainty in the $^3$He form factors (1.5%), and a 0.5% uncertainty due to possible fluctuations in the target density during the change of the beam energy from 4805.5 to 644 MeV.

Event triggers were formed by coincident signals from scintillator arrays. Particle tracks were reconstructed using the HRS vertical drift chambers. The small $\pi^-$ background in the HRS-L was rejected using a $CO_2$ Gas Čerenkov detector. In the HRS-R, coincident $\pi^+$, $^2$H, and $^3$H were separated from the protons using the time difference between particles detected in the two spectrometers. Most of the accidental coincident events were rejected by cuts on the difference between interaction points in the target along the beam as reconstructed by the two spectrometers, and on the $E_m$ (missing energy) spectrum. The remaining accidental background was subtracted using the coincidence timing between the spectrometers. Events originating in the target Al walls were rejected by requiring reconstructed events to originate within 3.5 cm from the target center.

In the cross-section analysis, a flat acceptance region of both HRSs was defined using a R-function cut imposed on the target variables. A R-function is a function whose sign is completely determined by the signs of its arguments [8, 9]. Using constructive-geometrical properties of R-functions, one can define a complicated multidimensional acceptance region as an analytical expression, and vary the region's boundaries until the phase space is maximized within the flat acceptance region of the spectrometers [10]. The use of R-functions allowed us to double the accepted phase space compared to the commonly used rectangular cuts on target variables.

The $^3$He$(e,e'p)d$ cross section was extracted using the simulation program MCEEP [11], taking into account the effects of internal and external radiation, particle energy loss, deviations from monochromaticity of the beam, and spectrometer resolutions. Simulated event yields were adjusted separately varying the $^3$He$(e,e'p)d$ and $^3$He$(e,e'p)pn$ cross sections in the simulation, until the simulated yield was equal to the detected yield in each $(E_m, p_m)$ kinematic bin [10]. Cross sections, averaged over each bin, were extracted from the re-weighted

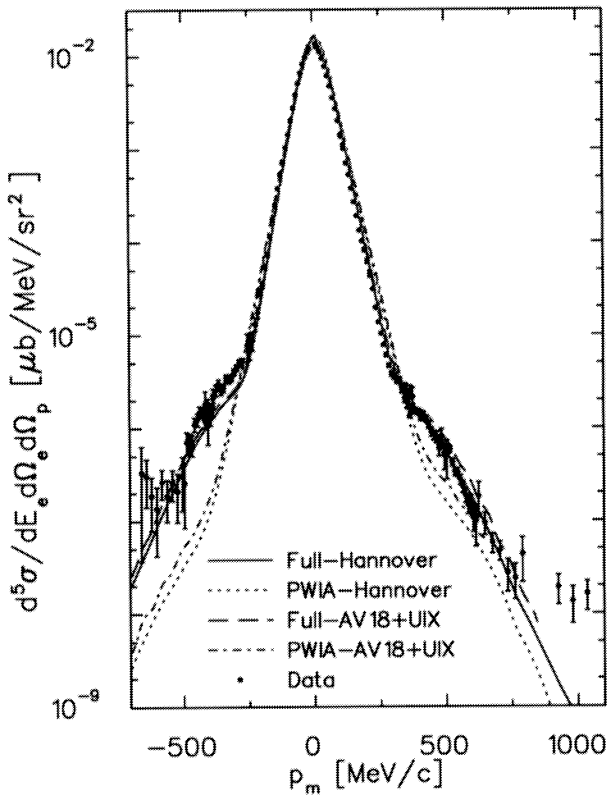


FIG. 1: Measured $^3$He$(e,e'p)d$ cross section as a function of the missing momentum, $p_m$. Negative (positive) $p_m$ correspond to protons detected left (right) of $\vec{q}$. Also displayed are two pairs of PWIA and full calculations by Laget. The two pairs differ in the ground-state wave function.

$^3$He$(e,e'p)d$ yield, corrected for radiation, and for contributions from $^3$He$(e,e'p)pn$ to each $^3$He$(e,e'p)d$ kinematic bin (on average, these contributions were about 3%). Within each bin, the simulated $^3$He$(e,e'p)$ cross section was assumed to depend on the $\sigma_{cc1}$ prescription of de Forest [12] for the off-shell electron-proton cross section. This technique allows one to separate the $p_m$ dependence of the reaction from the rapid dependence on the electron kinematics [10]. In addition to the over-all normalization uncertainty (2.9%, see above) the over-all systematic uncertainty was 3.4%, dominated by uncertainties in the solid angle (2.0%), the selection ($E_m$ cut) of the two-body break-up reaction channel (1.5%) and the knowledge of the effective target length via a cut on the interaction vertex location (1.4%).

The extracted $^3$He$(e,e'p)d$ cross section is plotted in Fig. 1 as a function of $p_m$. We note that the range of $p_m$ measured (resulting in measured cross-section magnitudes varying over six orders of magnitude), is significantly larger than in any other previous measurement. Moreover, contrary to previous experiments [13, 14, 15], our measurements over this entire range were performed at a fixed electron kinematics.

Also displayed in Fig. 1 are four theoretical curves by Laget. The Hannover calculations by Laget use the Hannover bound-nucleon wave function [16] corresponding to the solution to the three-body Faddeev equation with the Paris NN potential and no three-body forces. The AV18+UIX curves are the same PWIA and full calculations respectively, but with a bound-state nuclear wave function derived by a variational technique using the Argonne V18 NN potential and the Urbana IX three-body force [17]. All calculations use a diagrammatic approach. The kinematics as well as the nucleon and meson propagators are relativistic, and no restricted angular (Glauber type) approximation has been made in the various loop integrals. Details of the model can be found in [18]. The PWIA curves include only one-body interactions, while the full calculations include FSI, meson ($\pi$ and $\rho$) exchange and intermediate $\Delta$ formation currents as well as three-body (three nucleon $\pi$ double scattering) amplitudes. The FSI in these calculations follow a global parameterization of the NN scattering amplitude, obtained from experiments in LANL, SATURNE and COSY [19]. On this scale, the differences between the calculations using the two ground-state wave functions are very small. By far, FSI constitute the major difference between the full and PWIA calculations. Meson exchange and intermediate $\Delta$ current contributions are generally small (up to 20-25%), and the three-body contributions are negligible [19].

Three regions of $p_m$ can be discerned in Fig. 1. For $|\vec{p}_m|$ below $\sim$150 MeV/$c$, where the recoiling deuteron can be viewed as only marginally involved in the interaction, the data are expected to be dominated by the single-proton characteristics of the $^3$He wave function. As can be observed, both the PWIA and full curves describe the data quite well, and the difference between them is rather small. For $|\vec{p}_m|$ between 150 and 750 MeV/$c$, the cross section is expected to be dominated by the dynamics of the reaction. Indeed, very large contributions from dynamical effects are observed. While Laget's full calculations describe the data very well, the PWIA curve over- (under-) predicts the data by up to an order of magnitude for $|\vec{p}_m|$ below (above) 300 MeV/$c$. This difference between the two curves is very much dominated by FSI. At $x_B$=1, the on-shell rescattering of the fast nucleon on a nucleon at rest is preferred and the contribution of FSI is maximal. Because the NN scattering amplitude is almost purely absorptive in the JLab energy range, the corresponding FSI amplitude interferes destructively with the PWIA amplitude below, and constructively above $p_m \approx$300 MeV/$c$ [19]. For $p_m$ larger than 750 MeV/$c$, Laget's calculations gradually deviate from experimental data: at 1000 MeV/$c$, they grossly under-predict the measured cross section by more than an order of magnitude. Whether it is a consequence of the truncation of the diagrammatic expansion or a signature of other degrees of freedom is an open question.

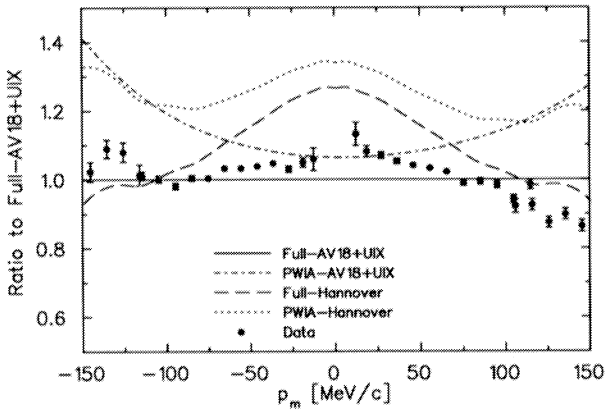


FIG. 2: Same data as in Fig. 1 for low $p_m$ only, but shown as a ratio to Laget's full calculations using the ground-state wave function (gswf) generated from the AV18 NN potential and the Urbana IX three-nucleon force. Also shown are the ratios of this calculation to Laget's full calculations that use the Hannover gswf, as well as the two corresponding PWIA curves.

The sensitivity of the data to the details of the wave function at low $|\vec{p}_m|$ is shown in Fig. 2. In order to enhance the details, Fig. 2 displays the low $|\vec{p}_m|$ subset of the data from Fig. 1 as a ratio to Laget's full calculations using the AV18 NN potential and the Urbana IX three-nucleon force. Also displayed are the ratios to the same calculations of Laget's full Hannover ground-state wave function and the two corresponding PWIA curves. As already noted, in the low $|\vec{p}_m|$ region, reaction effects such as FSI and two-body currents are relatively small as compared to higher $|\vec{p}_m|$ (Fig. 1), and the curves are mainly sensitive to the details of the bound-nucleon wave function. For $p_m$ below 50 MeV/$c$, the calculations are purely co-planar perpendicular kinematics whereas experimentally, because of the large $|\vec{q}|$, it is difficult to avoid contaminations with parallel and out-of-plane components. For $|\vec{p}_m| > 50$ MeV/$c$, we observe that the best agreement with the data is of the full AV18+UIX curve. We suggest that this better agreement with the data is related to the fact that the wave function generated from the AV18+UIX potentials reproduces the correct $^3$He binding energy, while the Hannover wave function that does not include three-body forces underbinds the $^3$He by $\sim$ 0.7 MeV.

The $A_{TL}$ asymmetry was extracted for $0 \leq |\vec{p}_m| \leq$ 660 MeV/$c$ according to

$$A_{TL} = \frac{\sigma_{right} - \sigma_{left}}{\sigma_{right} + \sigma_{left}}, \qquad (1)$$

where $\sigma_{right}$ and $\sigma_{left}$ are coplanar $^3$He$(e,e'p)d$ cross sections measured right and left of the transferred-momentum $\vec{q}$ direction. In the extraction of $A_{TL}$, the phase-space acceptances of kinematics bins on both sides of $\vec{q}$ were matched in $p_m$, $\omega$, and $|\vec{q}|$. The $A_{TL}$ observable downplays the significance of the ground-state wave function, by virtue of the ratio involved in its definition [20] and there exist indications that it is sensitive to relativistic effects [21] and to mechanisms that break the simple factorization scheme of PWIA cross sections [22].

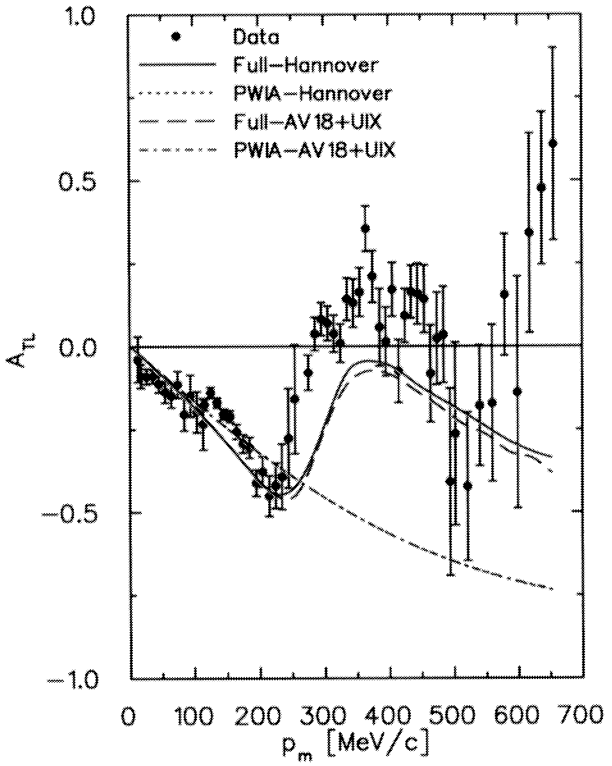


FIG. 3: The measured $A_{TL}$ asymmetry. The curves are the same four calculations by Laget used in Figs. 1 and 2; by definition, the two PWIA curves are indistinguishable.

Figure 3 displays the extracted $A_{TL}$ data with the PWIA and full calculations by Laget using the two ground-state wave functions described above. The difference in the two ground-state wave functions has a very small effect in the full calculations. In contrast to the PWIA calculations, the measured $A_{TL}$ displays a structure characteristic of broken factorization [22]: the oscillating pattern of $A_{TL}$ comes directly from the interference between different reaction amplitudes. Both of Laget's full calculations describe the data reasonably well by displaying similar structures. Such structure in $A_{TL}$ was previously observed in the quasielastic removal of p-shell protons in the $^{16}$O$(e,e'p)$ reaction [23], and was well reproduced by relativistic Distorted-Wave Impulse Approximation calculations by Udias *et al.* [24]. In that case, broken factorization was attributed to dynamical relativistic effects. However, these effects are marginal in our case because of the low nuclear density of $^3$He [25]. Rather, in our case, the factorization is broken because of the strong interference between the PWIA and

re-scattering amplitudes [19].

In summary, we measured the $^3$He$(e,e'p)d$ cross sections and $A_{TL}$ asymmetry at $Q^2 = 1.55$ GeV$^2$ and $x_B = 0.98$. For $|\vec{p}_m|$ below 150 MeV/$c$ the data are mostly sensitive to the details of the bound-nucleon wave function. The best agreement is observed with calculations using a $^3$He ground-state wave function generated from the Argonne V18 NN potential and the Urbana IX three-nucleon force, which also better reproduces the $^3$He binding energy. For $|\vec{p}_m|$ from 150 to 750 MeV/$c$, strong FSI effects are observed as quenching (enhancement) of the cross section below (above) $|\vec{p}_m|$ of about 300 MeV/$c$. For missing momenta from 750 to 1000 MeV/$c$, the measured $^3$He$(e,e'p)d$ cross sections are increasingly larger (more than an order of magnitude at 1000 MeV/$c$) than predicted by available theories. Whether it is a consequence of the truncation of the diagrammatic expansion or a signature of the existence of exotic effects is an open question. The measured $A_{TL}$ displays strong structure characteristic of broken factorization due to interference between the PWIA and re-scattering amplitudes. Calculations by Laget well describe all observables up to $|\vec{p}_m| = 750$ MeV/$c$. Other calculations of this reaction [25, 26, 27] that similarly interpret the data have recently become available.

This work was supported in part by the U.S. Department of Energy (DOE) contract DE-AC05-84ER40150 under which the Southern Universities Research Association (SURA) operates the Thomas Jefferson National Accelerator Facility, DOE contract DE-FC02-94ER40818, other DOE contracts, the National Science Foundation, the Italian Istituto Nazionale di Fisica Nucleare (INFN), the French Atomic Energy Commission and National Center of Scientific Research, the Natural Science and Engineering Research Council of Canada, and Grant-in-Aid for Scientific Research (KAKENHI) (No. 14540239) from the Japan Society for Promotion of Science (JSPS).

[1] A. Nogga, H. Kamada, and W. Gloeckle, Phys. Rev. Lett **85**, 944 (2000).
[2] A. Nogga, H. Kamada, W. Gloeckle, and B. R. Barrett, Phys. Rev. C **65**, 054003 (2002).
[3] J. Carlson and R. Schiavilla, Rev. Mod. Phys. **70**, 743 (1998).
[4] S. Frullani and J. Mougey, Adv. Nucl. Phys. **14**, 1 (1984).
[5] *Selected Studies of the $^3$He Nucleus through Electrodisintegration at High Momentum Transfer*, Jefferson Lab Experiment E89-044, M. Epstein, A. Saha and E. Voutier spokespersons.
[6] J. Alcorn et al., Nucl. Instru. and Meth. **A522**, 294 (2004).
[7] A. Amroun et al., Nucl. Phys. **A579**, 596 (1994).
[8] V. L. Rvachev and T. I. Sheiko, Appl. Mech. Rev. **48(4)**, 151 (1995).
[9] V. L. Rvachev, *Theory of R-functions and Some Applications* (Naukova Dumka, Kiev, Ukraine, 1982), in Russian.
[10] M. M. Rvachev, PhD thesis, MIT (2003).
[11] P. Ulmer, *MCEEP: Monte Carlo for Electro-Nuclear Coincidence Experiments, v.3.4* (2000).
[12] T. de Forest, Jr., Nucl. Phys. **A392**, 232 (1983).
[13] E. Jans et al., Phys. Rev. Lett. **49**, 974 (1982).
[14] C. Marchand et al., Phys. Rev. Lett **60**, 1703 (1988).
[15] R. Florizone et al., Phys. Rev. Lett. **83**, 2308 (1999).
[16] R. Schulze and P. Sauer, Phys. Rev. C **48**, 38 (1993).
[17] J. Forest et al., Phys. Rev. C **54**, 646 (1994).
[18] J.-M. Laget, Nucl. Phys. **A579**, 333 (1994).
[19] J.-M. Laget, Few Body Systems Supplement **15**, 171 (2003).
[20] J. J. Kelly, Adv. Nucl. Phys. **23**, 75 (1996).
[21] S. Gilad, W. Bertozzi, and Z. L. Zhou, Nucl. Phys. A **631**, 276c (1998).
[22] J. Udias, J. Javier, E. M. de Guerra, A. Escuderos, and J. Caballero, in *Proc. of the Vth Workshop on electromagnetic Induced Two-Hadron Emission* (2001), lund (Sweden), nucl-th/0109077.
[23] J. Gao et al., Phys. Rev. Lett **84**, 3265 (2000).
[24] J. Udias, J. Caballero, E. M. de Guerra, J. Amaro, and T. Donnelly, Phys. Rev. Lett. **84**, 5441 (1999).
[25] J. Udias, in *XXIII$^d$ International Workshop on Nuclear Theory* (2004), Rila (Bulgaria).
[26] C. C. degli Atti and L. Kaptari (2004), nucl-th/0407024.
[27] R. Schiavilla, O. Benhar, A. Kievsty, L. Marcucci, and M. Viviani (2004), to be published.